Orbit Based Estimation of Rewieved Jeffcott Model Dynamic Parameters for Rotating Machinery Powered by Suitable Electrical Networks.

Gerardo Peláez*, Filipe Tadeu, M.Donsión

1 Introduction.

2 Rotor orbit properties.

The first model proposal for an unbalanced flexible rotor dynamic analysis dates back to 1919 when Henry Hoffman Jeffcott developed a simple jet representative model based on a uniform flexible shaft over rigid bearings at its ends. The shaft mass plus the stage mass is concentrated at the shaft center. Based on this model Jeffcot was able to explain the violent vibration of the flexible rotor when the angular speed coincides with the natural frequency of the main rotating disk on its shaft elasticity, shown in Figure 1. If this the case the amplitude of the rotor vibration increases rapidily into this angular speed zone. The Jeffcot model includes both rotor displacements horizontal and vertical, that defines the orbit description or whole motion in the frequency domain that is briefly analysed in the following.

Regarding the Figure 2 the elastically restoring forces and the viscous damping forces are acting at point S. Thus the x and y components of Newtons second laws are

$$-kx - c\dot{x} = m(\ddot{x} - e_u\omega^2 cos(\omega t)) \tag{1}$$

*Corresponding Author, e-mail:*gpelaez@uvigo.es*

$$-ky - c\dot{y} = m(\ddot{y} - e_u\omega^2 sin(\omega t)) \tag{2}$$

where k_x states the stiffness of the rotor corresponding to the x-direction, k_y states the stiffness of the rotor corresponding to the y direction. Regarding the damping c_x and c_y also correspond to each direction. As it is customary Eqs (1-2) can be written in terms of the corresponding damping ratios and the natural frequencies of the x and y axis directions.

$$\zeta_x = \frac{c_x}{2\sqrt{k_x m}} \tag{3}$$

$$\zeta_y = \frac{c_y}{2\sqrt{k_y m}} \tag{4}$$

$$\omega_{nx} = \sqrt{\frac{k_x}{m}} \tag{5}$$

$$\omega_{ny} = \sqrt{\frac{k_y}{m}} \tag{6}$$

Thus by substituing Eqs. (3-6) into Eq (1) and (2) yields

$$\ddot{x} + 2\zeta_x\omega_{nx}^2 x = e_u\omega^2 cos(\omega t) \tag{7}$$

$$\ddot{y} + 2\zeta_y\omega_{ny}^2 y = e_u\omega^2 sin(\omega t) \tag{8}$$

At this point it is consider the most common case, namely, that of a shaft of circular cross section mounted over rolling elements bearings. If this is the case, the stiffness and damping are nearly the same in both directions x-y. Thus the two natural frequencies coincides and so do the damping ratio factors. Thus, Eq. (7) and (8) become

$$\ddot{x} + 2\zeta\omega_n^2 x = e_u\omega^2 cos(\omega t) \tag{9}$$

$$\ddot{y} + 2\zeta\omega_n^2 y = e_u\omega^2 sin(\omega t) \tag{10}$$

Recalling that a trigonometric function can be expressed in exponential form, and recognizing that e_u is a scalar, it is feasible to rewrite lumped together equations (9) and (10) by

$$\ddot{X}(t) + 2\zeta\omega_n\dot{X}(t) + \omega_n^2 X(t) = e_u\omega^2 e^{i\omega t} \tag{11}$$

with the understanding that, if the excitation is $e_u cos\omega t$, the response is

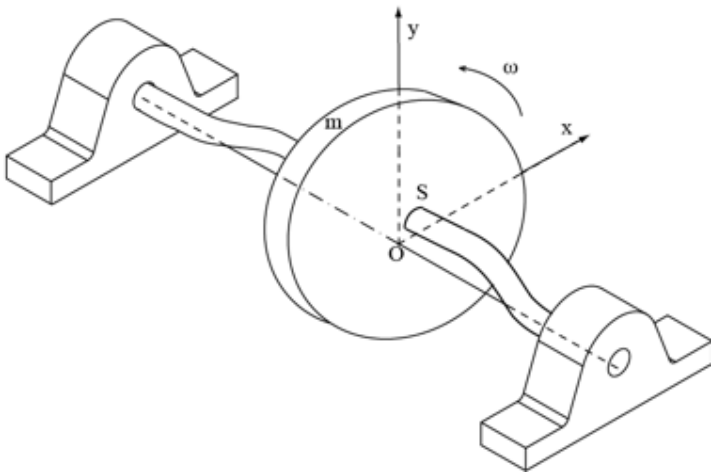

Figure 1: Flexible rotor over rigid bearings.

Re[X(t)] versus x(t) and if the excitation is $e_u sin\omega t$, the response is Img[X(t)] versus y(t). The advantage of the complex notation consist in that the solution of Eq. (9) and (10) is much more easy to obtain, than with real notation. In fact it is feasible to assume that the solution of Eq. (11) is of the form

$$X(t) = X(i\omega)e^{i\omega t} \tag{12}$$

with this assumption Eq.(11) becomes

$$[(\omega_n^2 - \omega^2) + 2\zeta\omega_n\omega i]X(i\omega)e^{i\omega t} = e_u\omega_n^2 e^{i\omega t} \tag{13}$$

thus,

$$X(i\omega) = \frac{\omega_n^2 e_u}{\omega^2 - \omega_n^2 + 2\zeta\omega\omega_n i} = \frac{e_u(\frac{\omega_n}{\omega})^2}{(1 - (\frac{\omega_n}{\omega})^2)) + i2\zeta\frac{\omega_n}{\omega}} \tag{14}$$

The main argument to describe the rotor response in terms of complex numbers notation consist in that it can give an interesting geometric translation. To this goal, let it be $X(i\omega) = x - iy$ a customary complex number, in addition $r = \frac{\omega_m}{\omega}$ states the frequency ratio between the assumed or modelled natural frequency and the actual rotation frequency ω. Note that the value anticipated by the Jeffcot model for the natural frequency should be

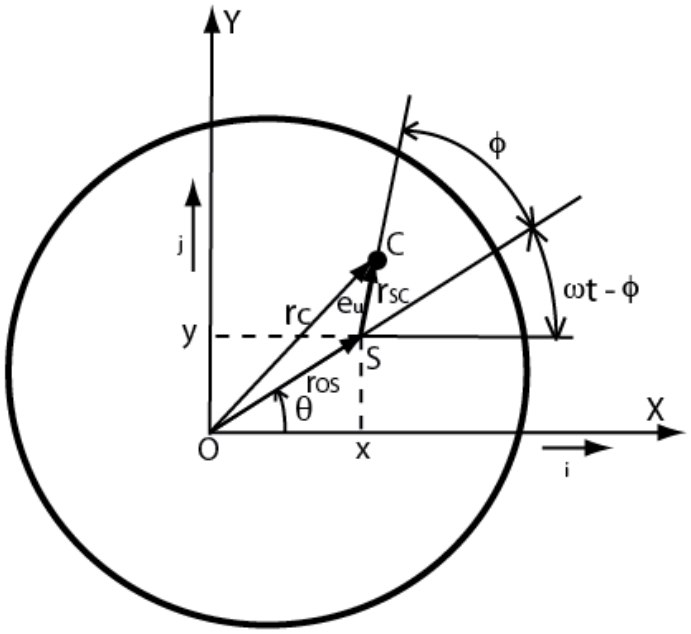

Figure 2: The rotor notable points. O:bearings centre, S:shaft centre where the elastic restoring force is applied, C:mass centre where the inertial force is applied,ϕ phase delay.

$\omega_n \simeq \omega_m = \sqrt{\frac{k}{m}}$ where $k = 48EI_z/\ell^3$ and m states the mass of the inertia disk. Finally without lost of generality allowing e_u be the unit Eq.(14) becomes

$$x - iy = \frac{r^2}{(1-r^2) + 2\zeta ri} \tag{15}$$

The use of algebraic manipulations expanding Eq.(15) as a function of the normalized frequency ration $q = 1/r$ gives

$$x(q^2 - 1) + 2\zeta yq = 1 \tag{16}$$

$$2\zeta xq - (q^2 - 1)y = 0 \tag{17}$$

Eliminating the parameter q between Eq.(16) and Eq.(17) can be done by first rewriting them as

$$(q^2 - 1) = \frac{1 - 2\zeta yq}{x} \tag{18}$$

$$(q^2 - 1) = \frac{2\zeta xq}{y} \tag{19}$$

it follows that

$$y - 2\zeta y^2 q = 2\zeta x^2 q \tag{20}$$

therefore

$$q = \frac{y}{2\zeta(x^2 + y^2)} \tag{21}$$

Substituing the q parameter value given by Eq (21) into Eq(16) yields

$$xy^2 - x(2\zeta(x^2 + y^2))^2 + 2\zeta y^2 + 2\zeta y^2 2\zeta(x^2 + y^2) = (2\zeta(x^2 + y^2))^2 \tag{22}$$

reordering terms and rejecting the null solution, Eq (22) becomes

$$y^2 - 4\zeta^2 x^4 - 8\zeta^2 x^2 y^2 - 4\zeta^2 y^4 - 4\zeta^2 y^2 x - 4\zeta^2 x^3 = 0 \tag{23}$$

At this point regarding the case $x \approx 0$ that implies $x^2 << y^2$, rejecting second order terms closed to zero Eq.(23) yields

$$y^2 - 4\zeta^2 y^4 - 4\zeta^2 y^2 x \simeq 0 \tag{24}$$

This a quadratic equation in y, again rejecting the trivial solution it simply becomes

$$1 \simeq 4\zeta^2(y^2 - x) \tag{25}$$

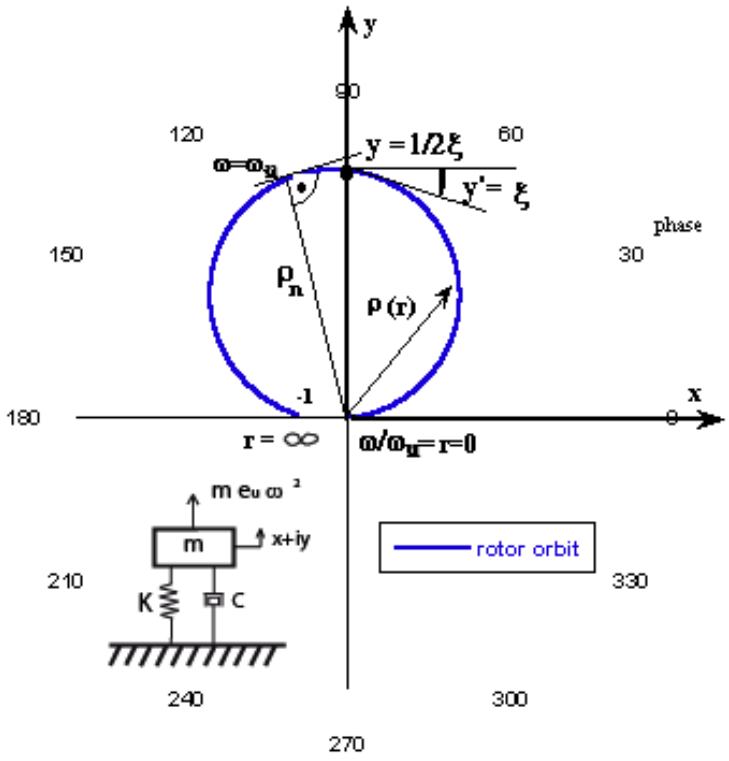

Figure 3: One hump theoretical rotor orbit.Conditions:ω_n =23.56 Hz, ζ = 0.1.

The Eq. (25) expresses a parabolae curve whose hump intersection with the y-axis is at the point $y = \frac{1}{2\zeta}$ and the slope value at such point is $\dot{y} = \zeta$, depicted in Fig. **??**. In view of this property it is feasible to extract the damping ratio from the theoretical rotor orbit. The rotor polar graph corresponds to the actual rotor radial deflection as the variation of the rotation speed progresses, in other correct terms, such polar graph states the orbit that the rotor undergoes around its rest position with reference to the embedded axis on it. As stated above the orbit shape its a function of damping ratio this is one of the orbit geometric properties quite valuables in order to identify the main parameters to build an accurate dynamic rotor model. Actually in a real world rotating machine orbit, several humps can take place. Each one corresponds to a resonant situation. And all of them lumped together build the whole rotating machine orbit. In addition each hump has it own orientation in the complex plane. Thus between each hump of a real world rotating

machine orbit and the theoretically orbit with only one hump depicted in Fig **??** the following differences can be found:

1. The parameters ρ and q involved by the theoretical orbit are dimensionless while the real world hump values: R the amplitude, and ω the frequency have dimensions.

2. With reference to initial and final points of the theoretical orbit, the actual orbit lacks such points or regions corresponding to the cases when ω equals zero and ω equals ∞ that can not be reached.

3. Actually each hump of the orbit is not placed at the theoretical orientation, its origin is arbitrary and it is a function other humps that the actual orbit migth have due to some nonlinearities between others.

4. In fact, the actual shape of one orbit hump can differ from the theoretical due to parasitic vibrations, nonlinearities plus measurement errors.

Anyway the availability of experimental reliable measurements corresponding to the rotor deflection R_i at the frequency ω_i are quite valuable in order to identify the rotating machine dynamic parameters. Note that the maximum deflection R_0 of the orbit hump is a reliable value, however the exact frequency at which it occurs $\omega_n$versus ω_0 have a quite valuable uncertainty associated due to the fast phase variation at such resonant region. In view of this, to analyticaly estimate the actual natural frequency of the whole rotating machine ω_n here is developed the following analysis. Let it be ρ_0 the maximum dimensionless rotor deflection amplitude that takes place at a inverse of the normalized frequency ration r_0 that must accomplish

$$\rho = \frac{r^2}{\sqrt{(1-r^2)^2 + 4\zeta^2 r^2}}; \left[\frac{d\rho}{dr}\right]_0 = 0 \tag{26}$$

From this point Maple 13 was used to carry out the values of r_0 and ρ_0 plus other symbolic computations

$$r_0 = \pm\frac{1}{\sqrt{1-2\zeta^2}} \tag{27}$$

the corresponding amplitude of vibration ρ_0 at this inverse of the frequency ratio r_0 is

$$\rho_0 = \frac{1}{(1-2\zeta^2)\sqrt{(1-\frac{1}{1-2\zeta^2})^2 + \frac{2\zeta^2}{1-2\zeta^2}}} \tag{28}$$

by simply substituing Eq.(27) into Eq.(28) yields,

$$\rho_0 = \frac{r_0^2}{\sqrt{(1-r_0^2)^2 + (2\zeta r_0)^2}} \tag{29}$$

thus as expected, the maximum dimensionless amplitude of vibration ρ_0 can be expressed as a function of its corresponding inverse normalized frequency ratio r_0. This verifies Eq.(15). Correspondingly any dimensionless amplitude of vibration ρ can be expressed in terms of its corresponding inverse normalized frequency ratio r plus only r_0, without involving the damping ratio ζ parameter.

$$\rho = \frac{r^2}{\sqrt{(1-r^2) + 2(r_0^2-1)(\frac{r}{r_0})^2}} \tag{30}$$

Or more likely in terms of the inverse of r, namely above the normalized frequency ratio $q = \omega/\omega_n$.

$$\rho = \frac{1}{q^2\sqrt{\frac{1}{q^4} - \frac{2q_0^2}{q^2} + 1}} \tag{31}$$

In the following this result will be used to solve the correlation between an experimental rotor orbit and the theoretical one synthesized on the basis of the assumed natural frequency ω_n and damping ratio ζ. Note however that the actual rotating machine global parameters can differ largely from the modelled ones. Between others, the contribution of the asynchronous motor inertia, stiffness and damping and its flexible coupling to the mechanical shaft will contribute to increase the uncertainty dealing with the global dynamic parameter associated to the Jeffcott rotating machine model initially proposed.

3 Estimation of the rotating machine dynamics parameters from its orbit.

In the following the correlation between the theoretical and the experimental rotor orbit will be solved to extract the actual dynamic parmeters from the experimental orbit. This will allow to build a more accurate rotating machine Jeffcot model.To this goal, as shown in Fig. **??**, let it be, the ratio between

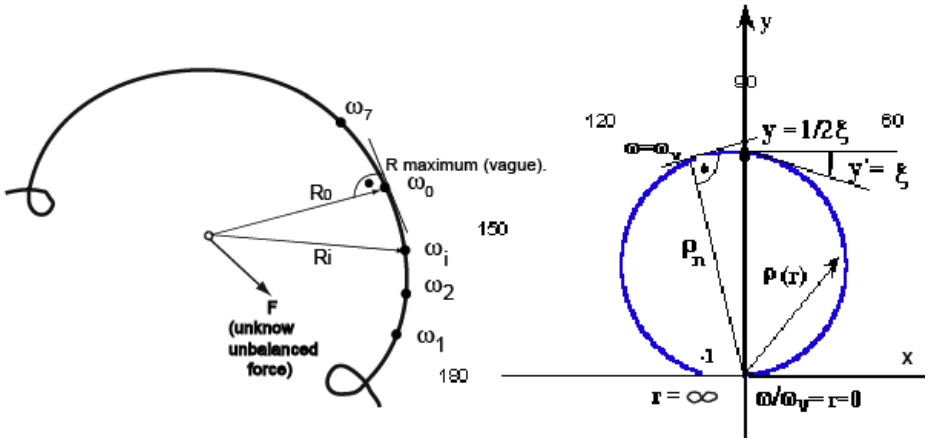

Figure 4: Skecth for comparision of actual and theoretical rotor orbit.

any experimentally measured amplitude of vibration R_i and the maximum measured amplitude R_0

$$\frac{R_i^2}{R_0^2} = \frac{1}{Z_i} \tag{32}$$

where the dimensionless parameter $N_i > 1$ states the inverse of such ratio. And for the R_i corresponding frequency ω_i, let it be

$$q_i^2 = q_0^2(1 + b_i) \tag{33}$$

where $q = \omega/\omega_n$ states again the normalized frequency. Thus Eq.(33) is equivalent to

$$b_i^2 = \frac{\omega_i^2 - \omega_0^2}{\omega_0^2} \tag{34}$$

where ω_0 states the actual global machine critical frequency. Looking forward the correlation between the experimental and the theoretical orbit we get

$$\frac{R_1}{\rho_1} = \frac{R_2}{\rho_2} = \cdots = \frac{R_i}{\rho_i} = \cdots = \frac{R_0}{\rho_0} \tag{35}$$

thus, according to Eq.(32) and (35) it can be written

$$\frac{R_i^2}{R_0^2} = \frac{\rho_i^2}{\rho_0^2} = \frac{1}{Z_i} \tag{36}$$

Where $Z_i = \frac{R_0^2}{R_i^2}$ is a dimensionless scalar. At this point substituing Eq.(31) into Eq.(36) yields,

$$\frac{\rho_i^2}{\rho_0^2} = \frac{1 - 2q_0^4 + q_0^2}{1 - 2q_0^2 q_i^2 + q_i^2} \tag{37}$$

combining Eq.(37),(36) and (33) gives,

$$\frac{1}{Z_i} = \frac{1 - q_0^4}{1 - q_0^4 + q_0^4 b_i^2} \tag{38}$$

rearranging terms, Eq.(38) becomes

$$b_i^2 = (Z_i - 1) \cdot \frac{1 - q_0^4}{q_0^4} \tag{39}$$

finally letting

$$Q = \frac{1 - q_0^4}{q_0^4} \tag{40}$$

where $q_0 = \frac{\omega_0}{\omega_m}$. Then the Eq.(39) can be simply rewritten as

$$b_i^2 = Q \cdot (Z_i - 1) \tag{41}$$

Shortly it has been found a linear relationship between b_i^2 and Z_i. Equation (41) provides an easy method for evaluating the actual critical frequency. The relevance of Eq.(41) can be explained by recalling that the prime concern Jeffcot modelled frequency $\omega_m = \sqrt{\frac{k}{m}}$ would differ from the actual global machine, mechanical shaft plus asynchronous motor, critical frequency ω_0.

a) Linear rotor. To demonstrate this assestment, a one stage rotating machine experimental frequency response was collected. The sketch of the machine is shown in Fig.5 and the measurements in table I.

$$\omega_0 = \omega_m \frac{1}{\sqrt[4]{1 + Q}} = ??\,[Hz] \tag{42}$$

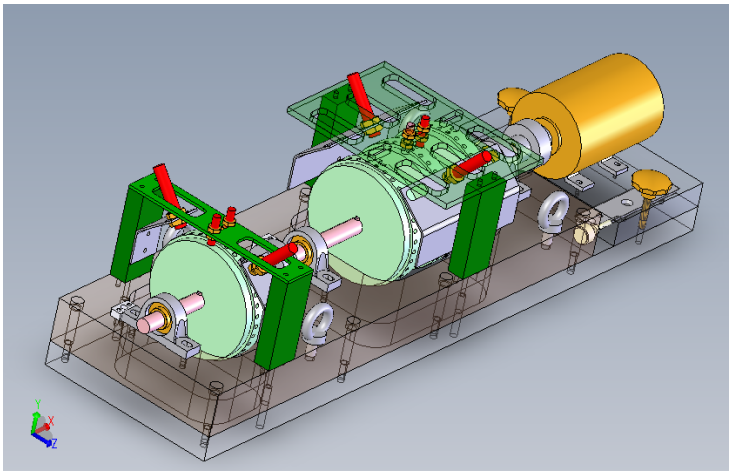

Figure 5: Experimental set up.

b) Non-linear keyed rotor. For the case of the keyed rotor and with reference to table II and figure 7 after the fitting process the slope of the linear polynomial was of around Q=0.11, thus

$$\omega_0 = \omega_m \frac{1}{\sqrt[4]{1+Q}} = 25.30\,[Hz] \tag{43}$$

Thus for the global rotating machine the frequency is ligthly shifted down due to the contribution of the asynchronuos motor inertia to the own mechanical shaft.

TABLE II

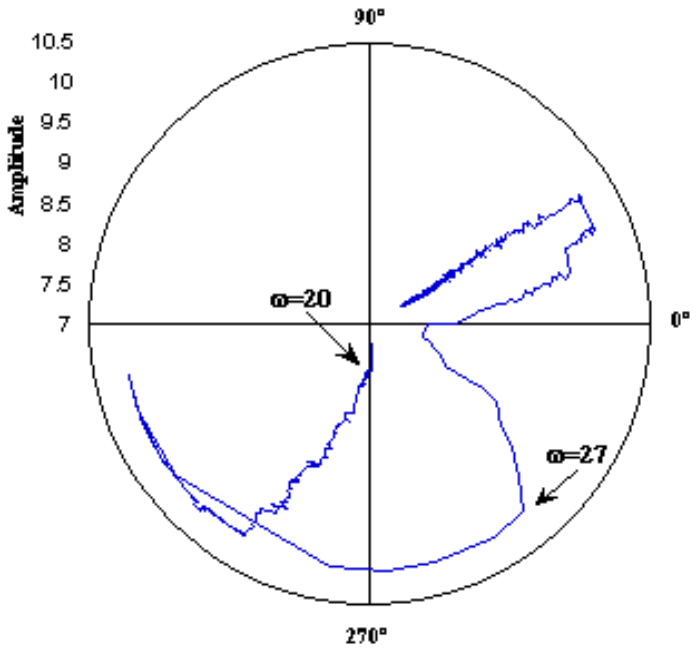

Figure 6: Experimental keyed rotor orbit.

i-input	R_i	ω_i	$b_i^2 = (\frac{\omega_i^2 - \omega_0^2}{\omega_0^2})$	$Z_i = \frac{R_0^2}{R_i^2}$
1	10.13	26.4061	0.0315	1
2	10.13	26.441	0.0342	1
3	10.0789	26.476	0.037	1.0102
4	10.0782	26.5252	0.0408	1.0103
5	10.0747	26.5393	0.0419	1.011
6	10.0785	26.5887	0.0458	1.0102
7	10.0805	26.6241	0.0486	1.0099
8	10.0779	26.6667	0.0519	1.0104
9	10.0769	26.7094	0.0553	1.0106
10	10.0776	26.7237	0.0564	1.0104
11	10.0798	26.7666	0.0598	1.01
12	10.0785	26.7953	0.0621	1.0102
13	10.0737	26.8528	0.0667	1.0112
14	10.0779	26.8962	0.0701	1.0104
15	10.076	26.9251	0.0724	1.0108
16	10.0798	26.9469	0.0742	1.01
17	10.0766	26.976	0.0765	1.0106
18	10.0798	27.049	0.0823	1.01
19	10.0769	27.0636	0.0835	1.0106
20	10.0744	27.1076	0.087	1.0111
21	10.0779	27.1444	0.09	1.0104
22	10.0776	27.2183	0.0959	1.0104
23	10.0763	27.2405	0.0977	1.0107
24	10.0766	27.1518	0.0906	1.0106
25	10.0637	27.0416	0.0817	1.0132
26	10.0554	27.1444	0.09	1.0149
27	10.0551	27.2702	0.1001	1.015
28	10.0557	27.3523	0.1067	1.0148
29	10.0541	27.4123	0.1116	1.0152
30	9.9916	27.4499	0.1146	1.0279
31	9.6466	27.4952	0.1183	1.1027
32	9.3347	27.5255	0.1208	1.1777
33	9.0656	27.5558	0.1233	1.2486
34	8.8338	27.5938	0.1264	1.315
35	8.6056	27.6243	0.1288	1.3857

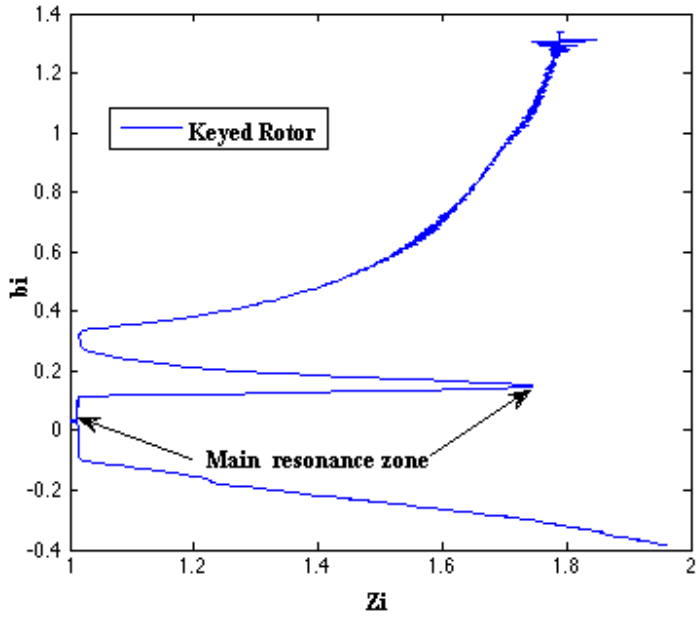

Figure 7: Evaluating critical frequency for the keyed rotor.

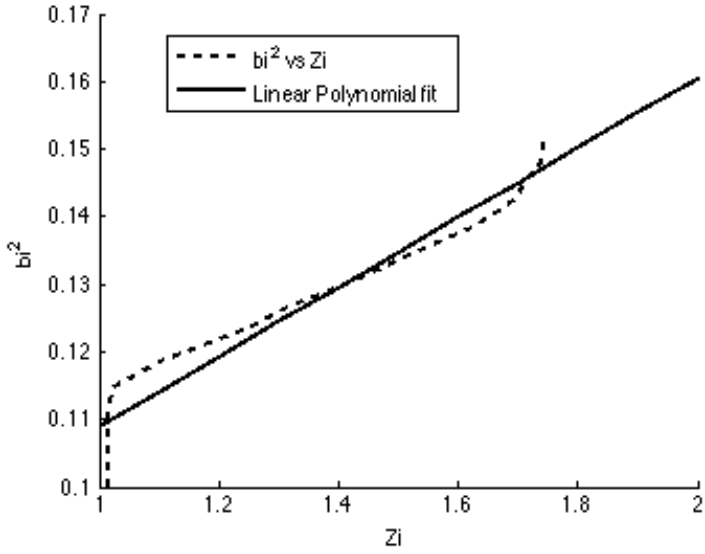

Figure 8: Main resonance zone: b_i^2 vs Z_i and the linear polynomial fitting.